Hard, soft and just right: variations in linked selection and recombination drive genomic divergence during speciation of aspens

Jing Wang[1], Nathaniel R. Street[2], Douglas G. Scofield[1,3,4], Pär K. Ingvarsson[1]

[1] Department of Ecology and Environmental Science, Umeå University, SE-90187, Umeå, Sweden

[2] Umeå Plant Science Centre, Department of Plant Physiology, Umeå University, SE-90187, Umeå, Sweden

[3] Department of Ecology and Genetics: Evolutionary Biology, Uppsala University, Uppsala, Sweden

[4] Uppsala Multidisciplinary Center for Advanced Computational Science, Uppsala University, Uppsala, Sweden

Corresponding author:

Dr Pär K. Ingvarsson, Department of Ecology and Environmental Science, Umeå University, Umeå, SE 90187, Sweden. Phone: +46907867414; Fax: +46-(0)-90-786-6705; E-mail: par.ingvarsson@emg.umu.se

Keywords: *Populus tremula*, *P. tremuloides*, Whole-genome re-sequencing, demographic histories, heterogeneous genomic differentiation, linked selection, recombination

Abstract

Despite the global economic and ecological importance of forest trees, the genomic basis of differential adaptation and speciation in tree species is still poorly understood. *Populus tremula* and *P. tremuloides* are two of the most widespread tree species in Northern Hemisphere. Using whole-genome re-sequencing data from 24 *P. tremula* and 22 *P. tremuloides* individuals, we find that the two species diverged ~2.2-3.1 million years ago. The approximately allopatric speciation of the two species was likely the results of the severing of the Bering land bridge combined with the onset of dramatic climatic oscillations throughout the Pleistocene. We detected moderate but also considerable heterogeneous genomic differentiation between species. Rather than being physically clustered into just a few large, discrete genomic 'islands' as may be expected when species diverges in the presence of gene flow, we found that the regions of differentiation were particularly steep, narrowly defined and located in regions with substantially suppressed recombination. It appears that species-specific adaptation, mainly involving standing genetic variation via soft selective sweeps, was likely the predominant proximate cause in generating the differentiation islands between species and not local differences in permeability of gene flow. In addition, we identified multiple signatures of long-term balancing selection predating speciation in regions containing immunity and defense-related genes in both species.

Introduction

Understanding how genomes diverge during the process of speciation is a central goal in evolutionary genetics (Nosil, et al. 2009; Strasburg, et al. 2012; Seehausen, et al. 2014). Under neutrality, differentiation is expected to accumulate as a result of the stochastic fixation of polymorphisms by genetic drift (Coyne and Orr 2004). Historical demographic processes can accelerate or decelerate the rate of differentiation through changes in the effective population sizes of nascent daughter species (Avise 2000). In general, both random genetic drift and demographic processes are expected to affect the entire genome (Luikart, et al. 2003). Natural selection, however, is expected to only influence those loci involved in ecological specialization and/or reproductive isolation, resulting in patterns of polymorphisms and divergence that deviate from neutral predictions in genomic regions under selection (Luikart, et al. 2003; Via 2009). The functional architectures of genomes, e.g. mutation and recombination rates, are also important factors in determining genomic landscape of differentiation (Noor and Bennett 2009; Nachman and Payseur 2012; Renaut, et al. 2013; Burri, et al. 2015). For instance, suppressed recombination can lead to increased differentiation by two mechanisms: preventing gene flow between species to avoid the break-up of co-adapted alleles, and the diversity-reducing effects of linked selection (Noor and Bennett 2009). A longstanding challenge in speciation genetics has been to quantify the relative contributions of various evolutionary forces in generating and shaping patterns of genomic divergence during speciation.

With the advance of next generation sequencing (NGS) technologies, a growing number of studies have found highly heterogeneous patterns of genomic

differentiation between recently diverged species (Feulner, et al. ; Turner, et al. 2005; Ellegren, et al. 2012; Renaut, et al. 2013; Carneiro, et al. 2014; Feulner, et al. 2015). A common explanation is that levels of gene flow between species differ across the genome, where increased genetic divergence in 'differentiation islands' is observed in a small number of regions supposed to contain loci involved in reproductive isolation ('speciation islands'), while the remainder of the genome is still permeable to ongoing gene flow and therefore shows lower levels of differentiation (Nosil, et al. 2009; Sousa and Hey 2013). However, some recent studies have argued that highly differentiated regions should represent 'incidental islands' that are not tied to the speciation processes, but result from the diversity-reduced effects of linked selection (either positive or purifying selection) (Noor and Bennett 2009; Turner and Hahn 2010; Nachman and Payseur 2012; Cruickshank and Hahn 2014). In contrast, long-term balancing selection is supposed to maintain stable trans-species polymorphisms and leave signatures of unusually low genetic differentiation between species (Charlesworth 2006). Under this scenario, heterogeneous selection alone is sufficient to generate patterns of heterogeneous genomic differentiation even in complete allopatry (Noor and Bennett 2009; Turner and Hahn 2010; White, et al. 2010). Exhaustive examination of the above two models is needed in more species and should preferably include details concerning the speciation processes, such as time of divergence, prevalence and rates of gene flow, well-characterized demographic histories and selective and recombination details (Nosil and Feder 2012).

Although largely understudied compared to other model species, forest trees represent a promising system to understand the genomic basis of species divergence and adaptive evolution; as a group they have developed diverse strategies to adapt and thrive across a wide range of climates and environments (Neale and Kremer 2011).

119 *Populus tremula* (European aspen) and *P. tremuloides* (American aspen) are two of
120 the most ecologically important and geographically widespread tree species of the
121 Northern Hemisphere (Figure 1a). Both are keystone species, display rapid growth,
122 high tolerance to environmental stresses, and long-distance pollen and seed dispersal
123 via wind (Eckenwalder 1996; Müller, et al. 2012). Based on their morphological
124 similarity and close phylogenetic relationships, they are considered sister species, or
125 less commonly, conspecific subspecies (Eckenwalder 1996; Wang, et al. 2013). They
126 can readily cross and artificial hybrids usually show high heterosis (Hamzeh and
127 Dayanandan 2004; Tullus, et al. 2012; Wang, et al. 2013). A recent study based on
128 several nuclear and chloroplast loci suggests that the first opening of the Bering land
129 bridge may have driven the allopatric speciation of the two species (Du, et al. 2015).

130 In accordance with their continent-wide distributions and broad ecological
131 ranges, *P. tremula* and *P. tremuloides* harbor among the highest levels of genetic
132 diversity found in plant species thus far (Wang, et al. unpublished data). The
133 extraordinary levels of genetic diversity in both species and the availability of a high-
134 quality reference genome in the congener, *P. trichocarpa* (Tuskan, et al. 2006), also
135 provide ideal opportunities to identify the relative roles that new mutations (hard
136 selective sweeps) versus pre-existing standing variations (soft selective sweeps) have
137 played during adaptive differentiation and speciation at the genome scale. In hard-
138 sweep models of adaptation, novel beneficial mutations arise and are rapidly fixed in
139 a species, and this process is expected to leave a signature of severely reduced
140 polymorphism in the vicinity of the beneficial mutation (Smith and Haigh 1974).
141 Models of adaptation via soft sweeps assume that beneficial alleles originate from
142 standing genetic variation or by recurrent independent novel mutations (Hermisson
143 and Pennings 2005). Given that the background variation of selectively advantageous

144 alleles is more heterogeneous in a soft sweep scenario, less severe reductions in levels
145 of polymorphism are expected for soft sweeps compared to hard sweeps (Hermisson
146 and Pennings 2005; Pennings and Hermisson 2006). Based on whole-genome re-
147 sequencing data in both *P. tremula* and *P. tremuloides*, our goals were to*:* (1) estimate
148 the species' divergence time and reconstruct demographic histories of the two species;
149 (2) infer and distinguish the relative roles of different evolutionary forces in
150 generating and shaping patterns of genomic differentiation between species; (3)
151 evaluate the relative importance of new mutations or standing genetic variation during
152 adaptive divergence in these widespread forest trees; and (4) identify genomic regions
153 and genes that may have evolved in response to directional and balancing selection
154 during speciation.
155

156 ## Results

157

158 We generated whole-genome sequence data for 24 *P. tremula* and 22 *P. tremuloides*,
159 and more than 88% of sequenced reads in each sample were aligned to the *P.*
160 *trichocarpa* reference genome (Table S1). The average coverage of uniquely mapped
161 reads per site was 25.1 and 22.5 in samples of *P. tremula* and *P. tremuloides*,
162 respectively (Table S1).
163

164 **Population structure**

165 The genome-wide NGSadmix analysis clearly sub-divided all sampled individuals
166 into two species-specific groups when the number of clusters was $K = 2$ (Figure 1b).
167 When $K = 3$, there was evidence for further population sub-structuring in *P.*
168 *tremuloides*, where individuals from populations originating in Alberta and Wisconsin

169 clustered into two subgroups. With K = 4, most *P. tremula* individuals were inferred
170 to be a mixture of two genetic components, showing slight clinal genetic variation
171 with latitude. No further structure was found when K = 5. A principal component
172 analysis (PCA) further supported these results (Figure 1c). Only the first two
173 components were significant (Table S2) based on a Tracy-Widom test, and these
174 explained, respectively, 21.4% and 2.1% of total genetic variance (Figure 1c). Among
175 the total number of polymorphisms between the two species, fixed differences
176 between *P. tremula* and *P. tremuloides* accounted for 1.1%, whereas 16.7% of
177 polymorphisms were shared between species, with the remaining polymorphic sites
178 being private in either of the two species (Figure 1d).

179 We examined the extent of population subdivision in *P. tremuloides* by
180 measured F_{ST} and d_{xy} between the two *P. tremuloides* populations (Alberta and
181 Wisconsin) along individual chromosomes (Table S3). We found low levels of
182 genetic differentiation (F_{ST}: 0.0443±0.0325) between the populations (Table S3).
183 Total sequence differentiation in the inter-population comparison (mean d_{xy} =
184 0.0165±0.0083) was similar to mean sequence differences in intra-population
185 comparisons ($\pi_{Alberta}$: 0.0161±0.0081; $\pi_{Wisconsin}$: 0.0157±0.0080, Table S3), indicating
186 that individuals of the two populations were genetically not more different from each
187 other than individuals within each population. Further tests based on the allele
188 frequency spectrum (Tajima's D and Fay & Wu's H) also supported these general
189 patterns (Table S3).

190

191 **Demographic histories**

192 We used *fastsimcoal2* (Excoffier, et al. 2013) to infer the divergence time between *P.*
193 *tremula* and *P. tremuloides* and their past demographic histories from the joint site

194 frequency spectrum. Eighteen divergence models were evaluated (Table S4), and the
195 best fit was provided by a simple isolation-with-migration model, where populations
196 of *P. tremuloides* experienced exponential growth while a stepwise population size
197 change occurred in *P. tremula* after the two species diverged (Figure 2a). The exact
198 parameter estimates of divergence time, migration rates, population sizes and their
199 associated 95% confidence intervals (CI) inferred from 100 parametric bootstraps are
200 given in Table 1. The estimated split time between *P. tremula* and *P. tremuloides*
201 (T_{DIV}) was ~2.3 million years ago (Mya) (bootstrap range [BR]: 2.2-3.1 Mya). The
202 contemporary effective population sizes (N_e) of *P. tremula* ($N_{P.tremula}$) and *P.*
203 *tremuloides* ($N_{P.tremuloides}$) were 102,814 (BR: 93,688-105,671) and 309,500 (BR:
204 247,321-310,105) respectively, with both being larger than the effective population
205 size of their common ancestor (N_{ANC} = 56,235 [48,012-69,492])). Gene flow ($2N_e m$,
206 where N_e is the effective population size and m is the migration rate) from *P.*
207 *tremuloides* to *P. tremula* was higher (0.202 migrants per generation [0.156-0.375])
208 than in the opposite direction (0.053 [0.052-0.117]). It was most likely due to the
209 higher N_e of *P. tremuloides* compared to *P. tremula* (Slatkin 1985), while the overall
210 migration rates in both directions were fairly low given the large N_e in both species
211 (Morjan and Rieseberg 2004). The low migration rates are not unexpected given the
212 large geographical distance and disjunct distributions between the two species.

213 The multiple sequential Markovian coalescent (MSMC)-estimated N_e for both
214 *P. tremula* (60,796) and *P. tremuloides* (49,701) at the beginning of species
215 divergence (around 2.3 Mya) were very similar to the *fastsimcoal2*-based estimates of
216 N_e for their ancestral population (Figure 2). Both species experienced similar
217 magnitudes of population decline following their initial divergence, and population
218 expansion in *P. tremuloides* began around 50,000-70,000 years ago and has continued

219 up to the present (Figure 2b). *P. tremula* experienced a substantial population
220 expansion following a longer bottleneck than that experienced by *P. tremuloides*
221 (Figure 2b).
222
223 **Genome-wide patterns of differentiation and molecular signatures of selection in**
224 **both high- and low-divergence regions**
225 We found that the majority of the genome showed moderate genetic differentiation,
226 with average F_{ST} value across the genome being 0.386 (see Figure 3a for the complete
227 distribution). Visual inspection indicates that genetic differentiation was
228 heterogeneous over 10 Kbp non-overlapping windows across the genome (Figure 4).
229 From the genome-wide empirical F_{ST} distribution, the cutoff for the top 2.5% highly
230 differentiated outlier windows was $F_{ST} > 0.681$ (Figure 3a). After removing windows
231 where d_{xy} values were lower than the genome-wide median (see Materials and
232 Methods), 461 out of 730 highly differentiated windows were retained (Figure 3b).
233 We based our analysis of genetic signatures of adaptation in these highly
234 divergent regions on our partitioning into categories that were likely to be under either
235 hard or soft selective sweeps based on levels of θ_π within each species (see Materials
236 and Methods; Figure 3b). A minority of outlier windows (5.87%) was consistent with
237 patterns expected for hard selective sweeps in both species (black dots in Figure 3b),
238 while somewhat more outlier windows showed signatures of having been influenced
239 by hard sweeps only in *P. tremula* (12.61%, red dots in Figure 3b) or *P. tremuloides*
240 (8.26%, blue dots in Figure 3b). Soft selective sweeps appear to have affected the
241 remaining 73.3% of divergent outlier regions in one or both species (grey dots in
242 Figure 3b). Compared to the rest of the genome, the divergent outlier regions were
243 characterized by multiple signatures of selection in both species regardless of the

244 specific category that they belong to (as defined above; $P<0.05$, Mann-Whitney U
245 test). These further signatures include significantly skewed allele frequency spectrum
246 towards rare alleles (more negative Tajima's D), increased high-frequency derived
247 alleles (more negative Fay & Wu's H), and stronger signals of linkage disequilibrium
248 (LD) (Table 2 and Figure S4). Divergent regions linked to soft sweeps showed
249 substantially weaker signatures of selection compared to those linked to hard sweeps,
250 with a much subtle excess of low-frequency alleles and weaker levels of LD (Table 2
251 and Figure S4a,c), but with comparable or even greater excesses of high-frequency
252 derived alleles (Table 2 and Figure S4b). Furthermore, we found that all highly
253 divergent regions showed significantly higher proportion of inter-species fixed
254 differences and lower proportion of inter-species shared polymorphisms compared to
255 the remainder of the genome (Table 2 and Figure S5 a-c). Even after correcting for
256 possible variation in the mutation rate among genomic regions (Feder, et al. 2005), we
257 found that relative node depths (RND) were significantly higher in divergent regions
258 associated with either hard or soft sweeps than the rest of the genome (Table 2 and
259 Figure S5d).

260 The cutoff for the bottom 2.5% of the empirical F_{ST} distribution, denoting
261 outlier windows of exceptionally low levels of interspecies divergence, was F_{ST} <
262 0.169 (Figure 3a). After excluding windows with coverage breadth lower than 3 Kbp
263 and retaining windows with high levels of polymorphisms in both species (see
264 Materials and Methods), we identified 49 outlier windows as candidate targets of
265 long-term balancing selection (green dots in Figure 3c). In contrast to the genomic
266 background, these candidate regions showed an excess of intermediate-frequency
267 alleles (higher Tajima's D and Fay & Wu's H values), and slightly lower levels of LD
268 (Table 2 and Figure S4). In addition, we found a negligible proportion of fixed

269 differences and significantly higher proportion of shared polymorphism in these
270 regions (Table 2 and Figure S5a-c). The higher RND values (Table 2 and Figure S5d),
271 however, were likely due to higher levels of ancestral polymorphisms that were
272 maintained by balancing selection before the two species split (Cruickshank and Hahn
273 2014).

274 Overall, candidate windows potentially under directional (both hard and soft
275 sweeps) or balancing selection were distributed across the genome (Figure 6). We
276 examined the physical sizes of these selected regions by combining adjacent windows
277 if they were all under selection. We found that the sizes of the selected regions all
278 appeared to be quite small, with the majority of selection likely occurring on a
279 physical scale smaller than 10 Kbp (Figure S6).

280

281 **Impact of recombination rate on patterns of genetic differentiation**

282 We examined relationships between population-scaled recombination rates (ρ) and
283 levels of inter-species divergence over non-overlapping 10 Kbp windows (Figure S7).
284 We found significant negative correlations between relative divergence F_{ST}, which
285 depends on genetic diversity within species, and population recombination rates in
286 both *P. tremula* (Spearman's ρ=-0.121, *P*-value<2.2e-16) and *P. tremuloides*
287 (Spearman's ρ=-0.157, *P*-value<2.2e-16) (Figure S7a). In contrast to F_{ST}, there were
288 significant positive correlations between absolute divergence d_{xy} and recombination
289 rates in both *P. tremula* (Spearman's ρ=0.199, *P*-value<2.2e-16) and *P. tremuloides*
290 (Spearman's ρ=0.140, *P*-value<2.2e-16) (Figure S7b).

291 Because $\rho=4N_e c$, where c is the per-generation recombination rate and N_e is
292 the effective population size, reduction of N_e in regions linked to selection will lower
293 local estimates of ρ even if local c is identical. In order to account for such effects, we

294 compared ρ/θ_π between regions with signals of selection and the rest of the genome,
295 because both ρ and θ_π are scaled by N_e. Relative to genomic background, our results
296 showed significantly suppressed recombination in all selected regions (Figure 5).
297
298 **Genes under selection**
299 The availability of an annotated *P. trichocarpa* genome enabled functional analyses
300 of candidate genes within regions that were putatively under selection. In total, 31
301 genes were located in divergent regions with signatures of hard sweeps in both
302 species (Table S5); 88 and 48 genes, respectively, were found in divergent regions
303 with signatures of hard sweeps only in *P. tremula* and *P. tremuloides* (Table S5), and
304 310 genes were located in highly differentiated regions with signatures of soft sweeps
305 in either one or both species (Table S5). Regions containing signatures of long-term
306 balancing selection contained a total of 80 genes (Table S6). Except for divergent
307 regions linked to soft sweeps where a significantly lower concentration of genes was
308 found ($P<0.001$, Mann-Whitney U test), all other selected regions showed comparable
309 gene densities compared to the rest of genome (Figure S8).
310 We used the Gene Ontology (GO) assignments of those candidate genes
311 putatively under selection to test whether specific GO terms were significantly over-
312 represented. After accounting for multiple comparisons, we did not detect any over-
313 representation for divergent regions with signatures of hard sweeps only in one
314 species or with signatures of soft sweeps. However, among genes with signatures of
315 hard sweeps in both species, we found 16 significantly enriched GO terms, mainly
316 including terms associated with transcription initiation and transcription factor
317 activity (Table S7). Within regions with signatures of long-term balancing selection,
318 21 significantly overrepresented GO terms were identified among the 80 candidate

319 genes (Table S8), with most of them being associated with immune response and
320 signal transduction.
321

322 ## Discussion

323

324 **Species divergence and demographic histories**

325 Our simulation-based analyses indicated that *P. tremula* and *P. tremuloides* diverged
326 around 2.2-3.1 Mya during the Late Pliocene and/or Early Pleistocene. This timing
327 corresponds closely with the first opening of the Bering Strait, which occurred 3.1-5.5
328 Mya and broke up the overland intercontinental migration route of terrestrial floras
329 between Eurasia and North America (Marincovich and Gladenkov 1999; Gladenkov,
330 et al. 2002). This may have been less of an immediate barrier to wind-dispersed
331 *Populus* than some other tree species, but the severing of the Bering land bridge
332 associated with the onset of dramatic climatic oscillations through the Pleistocene
333 were likely the principal drivers for initial divergence between *P. tremula* and *P.*
334 *tremuloides* (Comes and Kadereit 1998; Milne and Abbott 2002; Du, et al. 2015). We
335 found evidence of low gene flow between the two species following geographical
336 isolation, most likely due to the repeated opening and closing of the narrow strait
337 resulting from sea level fluctuations during the Quaternary glacial-interglacial cycles
338 (Hu, et al. 2010). Although these features of early divergence rule out a strictly
339 allopatric mode of speciation, given the modern-day large geographic isolation,
340 disjunct distributions and extremely low rates of gene flow, our results support an
341 approximately allopatric model of speciation for these two aspen species (Morjan and
342 Rieseberg 2004).

343 We found that the estimated effective sizes of current populations in both
344 species were larger than that of their ancestral population. The large contemporary N_e
345 of both species are in agreement with their wide geographic distributions and high
346 levels of genomic diversity (Wang, et al. unpublished data). The coalescent-based,
347 intra-species demographic analyses using MSMC also confirmed this pattern,
348 suggesting that both species have experienced substantial population expansion
349 following long-term population declines after divergence. Population expansion of *P.*
350 *tremuloides* occurred over the last 50,000-70,000 years, following the retreat of the
351 penultimate glaciation and continuing up to the present (Kaufman and Manley 2004).
352 *P. tremula*, in contrast, experienced a more extended population contraction.
353 Consistent with many other forest trees in Europe, the initiation of the substantial
354 expansion in *P. tremula* coincided with the end of the Last Glacial Maximum (Hewitt
355 2000; Hewitt 2004).
356 A possible caveat to our demographic inferences is the presence of population
357 subdivision in *P. tremuloides*. However, we found little genetic divergence and
358 similar patterns of genomic variation between the two subpopulations of *P.*
359 *tremuloides* (see Results), suggesting that subdivision may have occurred too recently
360 to influence our inferences of the speciation processes (Chikhi, et al. 2010). Similarly,
361 sampling could likely be more extensive in both species, to capture a greater extent of
362 the species-wide diversity but this is a perennial concern not restricted to our study.
363 Furthermore, inter-specific hybridization in either species is yet another potential bias.
364 However, there are no other species of *Populus* occurring in the regions from where *P.*
365 *tremula* were sampled. For *P. tremuloides*, naturally occurring hybridization is only
366 known to occur with *P. grandidentata* in central and eastern North America where the
367 two species co-occur (Pregitzer and Barnes 1980). Therefore any possible

368 hybridization in our study would be limited to samples from the Wisconsin population
369 of *P. tremuloides*, but as noted above we did not detect any major differences in
370 patterns of genetic variation between the two subpopulations suggesting little or no
371 effect of hybridization.
372
373
374 **Genome-wide patterns of differentiation between two widespread forest tree**
375 **species**
376 We detected moderate but also considerable heterogeneous genomic differentiation
377 between *P. tremula* and *P. tremuloides* (Figure 4). Stochastic genetic drift due to
378 geographical isolation has been proposed as the dominant evolutionary force driving
379 the overall patterns of genomic divergence between the two species (Coyne and Orr
380 2004). Complex demographic histories experienced by the two species also left
381 distinct patterns of genomic variation within and between species. The more dramatic
382 and/or longer period of range expansion in *P. tremuloides* resulted in genome-wide
383 excesses of low frequency alleles (negative Tajima's D) and the occurrence of more
384 private polymorphisms than in *P. tremula*. In contrast, the longer period of population
385 contraction experienced by *P. tremula* accelerated lineage sorting across the genome
386 due to reductions in effective population size (Fay and Wu 2000), which was
387 supported by the more negative values of Fay & Wu's H and the greater proportion of
388 derived fixed alleles in *P. tremula* relative to *P. tremuloides* (Table 2). Therefore, our
389 study suggests that neutral processes, e.g. drift and demographic history, were
390 responsible for the majority of genetic differentiation between the two aspen species
391 at a genome-wide scale (Strasburg, et al. 2012).

392 In addition to the overall pattern generated by these neutral processes, we
393 expected to find regions displaying exceptional differentiation ('differentiation
394 islands') that were characterized by multiple independent signatures of positive
395 selection in both species, including excesses of low-frequency alleles, increased high-
396 frequency derived alleles, increased LD, lower proportion of shared polymorphism
397 and/or higher proportion of fixed differences between species compared to the
398 genomic background. Rather than being physically clustered into just a few large,
399 discrete genomic 'islands', as expected when species diverge in the presence of gene
400 flow (Turner, et al. 2005), we found differentiation islands to be particularly steep,
401 narrowly defined and located in regions with substantially suppressed recombination
402 throughout the genome. Given the approximately allopatric mode of speciation we
403 envision for the two species, the differentiation islands most likely represent regions
404 harboring loci closely tied to species-specific adaptations rather than those resistant to
405 gene flow (Coyne and Orr 2004; Turner and Hahn 2010; Cruickshank and Hahn
406 2014). If natural selection is one of the main evolutionary forces shaping patterns of
407 genetic differentiation between these species, regions of low recombination would be
408 expected to show increased F_{ST} values, but not increased d_{xy} values (Noor and
409 Bennett 2009; Cruickshank and Hahn 2014). This occurs because natural selection
410 (through either selective sweeps and/or background selection) removes neutral
411 variation over longer distances in regions of low recombination (Begun and Aquadro
412 1992). As a consequence, relative measures of divergence (e.g. F_{ST}) that rely on
413 within-species diversity are expected to be higher in regions with restricted
414 recombination (Noor and Bennett 2009; Nachman and Payseur 2012). In contrast,
415 increased absolute divergence (e.g. d_{xy}) is only expected if reduced gene flow
416 occurred in regions of low recombination (Nachman and Payseur 2012). In

417 accordance with this view, we observed significant negative relationships between
418 population-scaled recombination rates (ρ) and F_{ST}, but not d_{xy}, in both species (Noor
419 and Bennett 2009; Keinan, et al. 2010).

420 Taken together, our findings highlight a significant effect of linked selection
421 in generating the heterogeneous differentiation landscape across the genome (Noor
422 and Bennett 2009; Turner and Hahn 2010; Nachman and Payseur 2012; Cruickshank
423 and Hahn 2014).

424

425 **Implications for understanding the genetic basis of adaptive evolution**

426 Patterns of polymorphism and divergence around adaptive sites would allow us to
427 study the degree to which adaptation occurred from new beneficial mutations (hard
428 selective sweeps) or from standing genetic variation (soft selective sweeps) (Pritchard,
429 et al. 2010). Population genetic theory predicts that soft sweeps are common in
430 organisms with large population sizes, because adaptation would not be limited by the
431 availability of beneficial mutations and should proceed primarily from standing
432 genetic variation (Hermisson and Pennings 2005). Accordingly, in forest tree species
433 with large distribution ranges and broad ecological niches, adaptation would seem to
434 be more likely to occur via soft sweeps (Barton and Malik 2010). We found that the
435 large majority (73%) of highly differentiated regions due to adaptive divergence
436 between the two species showed signatures of soft sweeps, but notably 27% of highly
437 differentiated regions showed signatures of hard sweeps in either one or in both aspen
438 species. It has been suggested that regions flanking hard sweeps or regions affected
439 by older hard sweeps could be misidentified as soft sweeps because they may produce
440 spurious population genetic signatures resembling soft sweeps (Schrider, et al. 2015).
441 Rather than occurring in the "shoulders" of completed hard sweeps, we found that

442 most regions with signatures of soft sweeps were distributed across the genome
443 without any association to regions linked to hard sweeps (Figure 4). In addition, we
444 found comparable and even more negative values of Fay & Wu's H in candidate
445 regions linked to soft sweeps compared to those linked to hard sweeps, suggesting
446 that soft selective sweeps are either incomplete or are still ongoing in many of these
447 regions (Fay and Wu 2000). The signals we observed are thus not likely to be a by-
448 product of older hard selective sweeps (Schrider, et al. 2015). Overall, our results
449 suggest that both hard and soft sweeps have been independently involved in divergent
450 adaptation between *P. tremula* and *P. tremuloides* (Pritchard and Di Rienzo 2010).

451 In comparison to divergent selection, long-term balancing selection maintains
452 stable trans-species polymorphisms and leave signatures of unusually low genetic
453 differentiation between species (Charlesworth 2006). We identified a number of
454 genomic regions that are potentially under long-term balancing selection in both *P.*
455 *tremula* and *P. tremuloides.* Apart from low inter-species divergence and high intra-
456 species diversity, these regions are characterized by several other signatures of
457 balancing selection, such as excesses of sites at intermediate frequencies, greater
458 proportions of shared polymorphisms between species and lack of fixed inter-species
459 differences. Due to the long-term effects of recombination on old balanced
460 polymorphisms (Leffler, et al. 2013), we found the signatures and footprints left by
461 balancing selection were generally much narrower and restricted compared to regions
462 under divergent selection, producing comparable or even lower levels of LD than we
463 observed for the rest of the genome. However, after accounting for the influence of
464 local N_e by measuring ρ/θ_π, we found significantly reduced recombination rates in
465 these regions relative to genome-wide averages, indicating that suppressed

466 recombination is likely to be critical to the maintenance of beneficial trans-species
467 polymorphisms over long evolutionary time scales (Kamau and Charlesworth 2005).
468
469 **Candidate genes and functions**
470
471 We were interested in exploring the functional commonalities of candidate genes
472 within regions putatively under either directional or long-term balancing selection in
473 *P. tremula* and *P. tremuloides*. For candidate genes located in highly differentiated
474 regions, no functional over-representation was found in genes linked to either soft
475 sweeps or species-specific hard sweeps. This indicates that a wide range of genes and
476 functional categories are likely to be involved in rapid adaptation in these widespread
477 species (Wolf, et al. 2010). We only found significant enrichment of GO for genes
478 where hard selective sweeps may have occurred in both species. These genes are
479 mainly associated with transcription initiation and transcription factor activity,
480 suggesting that beneficial mutations affecting transcriptional regulation are likely to
481 be a common source of adaptive evolutionary change between recently diverged
482 species (Wittkopp and Kalay 2012). Regions carrying signatures of long-term
483 balancing selection were enriched for genes involved in signal transduction, immune
484 and defense response. It highlights the influence of co-evolutionary arms races
485 between hosts and natural enemies on the persistence of functional genetic diversity
486 in immunity and defense-related genes (Tiffin and Moeller 2006; Salvaudon, et al.
487 2008). Future studies of these candidate genes are needed to better assess the adaptive
488 genetic potential of these two widespread forest tree species, and to predict how they
489 might respond to current and future climate.
490

Conclusion

We have provided insights into the recent evolutionary histories and speciation process separating the two closely related forest tree species, *P. tremula* and *P. tremuloides*. Consistent with the approximately allopatric mode of speciation, we detected moderate levels of genomic differentiation between the two species, and genomic regions of pronounced differentiation were found distributed throughout the genome at many small, independent locations, rather than being clustered into a few large genomic "islands", as is expected under a model of speciation-with-gene flow. Stochastic genetic drift and historical demographic processes have shaped patterns of polymorphism and differentiation at a genome-wide scale in both species. In addition, we found that species-specific adaptation, mainly involving standing genetic variation via soft selective sweeps, was likely the predominant proximate cause generating the differentiation islands between species, rather than local differences in permeability to gene flow. We must note that this adaptation may largely be unrelated to the speciation process. We also identified multiple signatures of long-term balancing selection in regions of exceptionally low differentiation that appear to have predated speciation. Our study thus highlights that future work should integrate more information on the natural histories of speciation, such as divergence time, geographical context, gene flow magnitudes, demographic histories and sources of adaptation when interpreting the meaning of observed genomic patterns of divergence between closely related species.

Materials and Methods

516 **Population samples, sequencing, quality control and mapping**

517 The analysis workflow of this study is shown in Figure S1. We extracted genomic
518 DNA from leaf samples of 24 genotypes in *P. tremula* and 22 genotypes in *P.*
519 *tremuloides* (Figure 1a and Table S1). We then constructed 2×100 bp paired-end
520 sequencing libraries with target insert sizes of 650bp for all genotypes that were
521 sequenced on the Illumina HiSeq 2000 platform at the Science for Life Laboratory in
522 Stockholm, Sweden. All samples were sequenced to a target coverage of 25X. The
523 sequencing data have been deposited in the Short Read Archive (SRA) at NCBI under
524 accession IDs ranging from XXXXXX-XXXXXX. The same dataset was also used in
525 (Wang, et al. unpublished data).

526 For all raw sequencing reads (Wang, et al. 2015), we used Trimmomatic
527 (Lohse, et al. 2012) to remove adapter sequences and cut off bases from either the
528 start or the end of reads when the base quality was lower than 20. Reads were
529 completely discarded if there were fewer than 36 bases remaining after trimming. We
530 then mapped all reads to the *P. trichocarpa* reference genome (v3.0) (Tuskan, et al.
531 2006), with default parameters implemented in bwa-0.7.10 using the BWA-MEM
532 algorithm (Li 2013). Local realignment was performed to correct for the mis-
533 alignment of bases in regions around insertions and/or deletions (indels) using
534 RealignerTargetCreator and IndelRealigner in GATK v3.2.2 (DePristo, et al. 2011).
535 In order to account for the occurrence of PCR duplicates introduced during library
536 construction, we used MarkDuplicates in Picard (http://picard.sourceforge.net) to
537 remove reads with identical external coordinates and insert lengths. Only the read
538 with the highest summed base qualities was kept for downstream analyses.

539

540 **Data filtering and genotype calling**

541 Prior to variant and genotype calling, we employed several filtering steps to exclude
542 potential errors caused by paralogous or repetitive DNA sequences. First, after
543 investigating the empirical distribution, we removed sites showing extremely low
544 (<100 reads across all samples per species) or high (>1200 reads across all samples
545 per species) read coverage. Second, as a mapping quality score of zero is assigned for
546 reads that could be equally mapped to multiple genomic locations, we removed sites
547 containing more than 20 such reads among all samples in each species. Third, we
548 removed sites that overlapped with known repeat elements as identified by
549 RepeatMasker (Tarailo-Graovac and Chen 2009). After all filtering steps, there were
550 42.8% of sites across the genome left for downstream analyses. Among them, 54.9%
551 were found within gene boundaries, and the remainder (45.1%) was located in
552 intergenic regions.

553 Two alternative bioinformatics approaches were then used (Figure S1): (1) For
554 those population genetic statistics that relied on the inferred site-frequency-spectrum
555 (SFS), estimation was performed directly from genotype likelihoods without calling
556 genotypes (Nielsen, et al. 2011), as implemented in ANGSD (Korneliussen, et al.
557 2014). Only reads with a minimal mapping quality of 30 and bases with a minimal
558 quality score of 20 were considered. For all filtered sites in both species, we defined
559 the alleles that were the same as those found in the *P. trichocarpa* reference genome
560 as the ancestral allelic state. We used the -doSaf implementation to calculate the site
561 allele frequency likelihood based on the SAMTools genotype likelihood model in all
562 sites (Li, et al. 2009), and then used the –realSFS implementation to obtain a
563 maximum likelihood estimate of the unfolded SFS using the Expectation
564 Maximization (EM) algorithm (Kim, et al. 2011). Several population genetic statistics
565 were then calculated based on the global SFS (Figure S1). (2) For those estimations

566 that required accurate genotype calls, single nucleotide polymorphisms (SNPs) and
567 genotypes were called with HaplotypeCaller in GATK v3.2.2 (Figure S1). A number
568 of filtering steps were performed to reduce false positives from SNP and genotype
569 calling: (1) Removed SNPs overlapping sites that did not pass all previous filtering
570 criteria; (2) Removed SNPs with more than 2 alleles in both species; (3) Removed
571 SNPs at or within 5bp from any indels; (4) Assigned genotypes as missing if their
572 quality scores (GQ) were lower than 10, and then removed SNPs with more than two
573 missing genotypes in each species. (5) Removed SNPs showing significant deviation
574 from Hardy-Weinberg Equilibrium (P<0.001) in each species. In total, we identified
575 5,894,205 and 6,281,924 SNPs passing these criteria across the 24 *P. tremula* samples
576 and 22 *P. tremuloides* samples, respectively.
577
578 **Population structure**
579 Population genetic structure was inferred using the program NGSadmix (Skotte, et al.
580 2013), which takes the uncertainly of genotype calling into account and works
581 directly with genotype likelihoods. Only sites with lower than 10% missing data were
582 used. We first used the SAMTools model (Li, et al. 2009) in ANGSD to estimate
583 genotype likelihoods and then generated a beagle file for the subset of the genome
584 that was determined as being variable using a likelihood ratio test (P-value $<10^{-6}$)
585 (Kim, et al. 2011). We predefined the number of genetic clusters K from 2-5, and the
586 maximum iteration of the EM algorithm was set to 10,000.
587 As another method to visualize the genetic relationships among individuals,
588 we performed principal component analysis (PCA) using ngsTools, which accounts
589 for sequencing errors and uncertainty in genotype calls (Fumagalli, et al. 2014). The
590 expected covariance matrix across pairs of individuals from both species was

591 computed based on the genotype posterior probabilities across all filtered sites.
592 Eigenvectors and eigenvalues from the covariance matrix were generated with the R
593 function eigen, and significance levels were determined using the Tracy-Widom test
594 as implemented in EIGENSOFT version 4.2 (Patterson, et al. 2006).
595
596 **Demographic history**
597 To infer demographic history associated with speciation of *P. tremula* and *P.*
598 *tremuloides*, we used a coalescent simulation-based method implemented in
599 *fastsimcoal* 2.5.1 (Excoffier, et al. 2013). We calculated two-dimensional joint site
600 frequency spectrum (2D-SFS) from posterior probabilities of sample allele
601 frequencies by ngsTools (Fumagalli, et al. 2014). 100,000 coalescent simulations
602 were used for the estimation of the expected 2D-SFS and log-likelihood for a set of
603 demographic parameters in each model. Global maximum likelihood estimates for
604 each model were obtained from 50 independent runs, with 10-40 conditional
605 maximization algorithm cycles, as implemented in *fastsimcoal* 2.5.1. Eighteen
606 divergence models were examined (Figure S2). All models began with the split of the
607 ancestral population into two sub-populations and differed in terms of (i) whether
608 post-divergence gene flow was present or not, (ii) levels and patterns of gene flow
609 between the two species, and (iii) how population size changes occurred, either at the
610 time of species divergence or afterwards (Figure S2). Model comparison was based
611 on the maximum value of likelihood over the 50 independent runs using the Akaike
612 information criterion (AIC) and Akaike's weight of evidence (Excoffier, et al. 2013).
613 The model with the maximum Akaike's weight value was chosen as the optimal one.
614 We assumed a mutation rate of 2.5×10^{-9} per site per year in *Populus* (Koch, et al.
615 2000) and a generation time of 15 years when converting estimates to units of years

616 and individuals. Parameter confidence intervals of the best model were obtained by
617 100 parametric bootstraps, with 50 independent runs in each bootstrap.
618 We then employed a newly developed multiple sequential Markovian
619 coalescent (MSMC) method (Schiffels and Durbin 2014), which is an extension of a
620 pairwise sequential Markovian coalescent (PSMC) method (Li and Durbin 2011), to
621 estimate variation of scaled population sizes (N_e) over historical time in both species.
622 Prior to the analysis, all segregating sites within each species were phased and
623 imputed using fastPHASE v1.4.0 (Scheet and Stephens 2006). Because MSMC
624 measures the time to the first coalescence between all pairs of haplotypes, resolution
625 for recent population size changes can be enhanced if more haplotypes are used
626 (Schiffels and Durbin 2014). We applied MSMC to phased whole-genome sequences
627 from one (two haplotypes), two (four haplotypes) and four (eight haplotypes)
628 individuals in each species, respectively. We did not include more haplotypes because
629 of the high computational cost of greater samples. A generation time of 15 years and a
630 rate of 2.5×10^{-9} mutations per nucleotide per year (Koch, et al. 2000) were used to
631 covert the scaled times and population sizes into real times and sizes.
632
633 **Genome-wide patterns of differentiation**
634 Because linkage disequilibrium (LD) decays within 10 kilobases (Kbp) in both *P.*
635 *tremula* and *P. tremuloides* (Wang, et al. unpublished data), we divided the genome
636 into 39,406 non-overlapping windows of 10 Kbp in size to investigate patterns of
637 genomic differentiation between species. For a window to be included in the
638 downstream analyses, we required there to be at least 1 Kbp sites left after all above
639 filtering steps. Levels of genetic differentiation between species at each site were
640 estimated using method-of-moments F_{ST} estimators implemented in ngsFST from the

641 ngsTools package (Fumagalli, et al. 2014), which calculates indices of the expected
642 genetic variance between and within species from posterior probabilities of sample
643 allele frequencies, without relying on SNP or genotype calling (Fumagalli, et al.
644 2013). We then averaged F_{ST} values of all sites within each 10 Kbp non-overlapping
645 window.

646 We defined outlier windows of exceptionally high interspecies divergence as
647 windows above the top 2.5% of the F_{ST} empirical distribution. As F_{ST} is a relative
648 measure of differentiation and is sensitive to intra-species genetic variation
649 (Charlesworth 1998; Cruickshank and Hahn 2014), we calculated another measure of
650 differentiation, d_{xy}, which is the pairwise nucleotide divergence between species and
651 that is independent of within-species diversity (Nei 1987). d_{xy} was calculated from
652 sample allele frequency posterior probabilities at each site using ngsStat from
653 ngsTools software package (Fumagalli, et al. 2014), and was then averaged over non-
654 overlapping 10 Kbp windows. Regions with high F_{ST} but low d_{xy} are more likely to be
655 caused by low ancestral polymorphism at times pre-dating speciation (Cruickshank
656 and Hahn 2014), therefore we retained only those outlier windows with d_{xy} values
657 higher than the genome-wide median value.

658 We identified windows below the bottom 2.5% of the F_{ST} empirical
659 distribution as outlier windows of exceptionally low levels of interspecies divergence.
660 Through further screening, we found a skewed pattern of low coverage breadth in
661 lowly differentiated windows compared to the genomic background and the highly
662 diverged windows (Figure S3). There is thus the possibility that regions showing low
663 genetic differentiation may contain some artifacts arising from mis-aligned reads due
664 to repetitive sequences or paralogs, despite the stringent quality filters we have

665 imposed. We thus performed another more stringent filtering on these regions by only
666 retaining windows with at least 3 Kbp sites left from previous quality filtering steps.
667
668 **Molecular signature of selection in high- and low-divergence regions**
669 To assess directional selection in highly divergent regions, we considered both hard-
670 and soft-sweep models. We calculated levels of genetic polymorphism (θ_π) using an
671 empirical Bayes approach with the maximum likelihood of unfolded SFS as a prior in
672 ANGSD, within each 10 Kbp non-overlapping window (Kim, et al. 2011). Because
673 hard sweeps would leave a signature of more severe reductions in levels of
674 polymorphism compared to soft sweeps (Hermisson and Pennings 2005; Pennings
675 and Hermisson 2006), a 5% threshold of θ_π was applied for outlier windows of
676 exceptional differentiation to classify divergent regions into four mutually exclusive
677 categories: (1) hard selective sweeps occurred in both species if θ_π dropped below the
678 bottom 5% of empirical distribution in both species; (2) and (3) hard selective sweeps
679 occurred in only one of *P. tremula* or *P. tremuloides* if θ_π dropped below the bottom 5%
680 of empirical distribution only in the respective species; (4) adaptations occurred from
681 standing genetic variation (soft selective sweeps) if θ_π appeared similar to background
682 levels (not below the threshold). In contrast to directional selection, one of the
683 strongest signatures of long-term balancing selection is an excess of polymorphism
684 surrounding the target of selection (Charlesworth 2006). We considered outlier
685 windows with exceptionally low F_{ST} values as potentially being subject to long-term
686 balancing selection if θ_π were in the top 5% of the empirical distribution in both
687 species.
688 We compared different unions of outlier windows to the remaining portion of
689 the genome by a variety of additional population genetic statistics in both species.

690 First, Tajima's D (Tajima 1989) and Fay & Wu's H (Fay and Wu 2000) were
691 calculated from sample allele frequency likelihoods in ANGSD. Second, levels of LD
692 and population-scaled recombination rates (ρ) were estimated based on the SNP data
693 created by GATK. To evaluate levels of LD within each 10 Kbp window, the
694 correlation coefficients (r^2) between SNPs with pairwise distances larger than 1 Kbp
695 were calculated using VCFtools v0.1.12b (Danecek, et al. 2011). Population-scaled
696 recombination rates $\rho = 4N_e c$ (Where N_e is the effective population size and c is the
697 recombination rate) were estimated using the Interval program of LDhat 2.2 (McVean,
698 et al. 2004) with 1,000,000 MCMC iterations sampling every 2,000 iterations and a
699 block penalty parameter of five. The first 100,000 iterations of the MCMC iterations
700 were discarded as burn-in. Resulting estimates of r^2 and ρ were averaged over each 10
701 Kbp window. In any of the two species, windows were discarded in the estimation of
702 r^2 and ρ if there were less than 3 Kbp and/or 10 SNPs left from previous filtering
703 steps. Finally, we used the program ngsStat (Fumagalli, et al. 2014) to calculate
704 another three measures of genetic differentiation in each window: with *P. trichocarpa*
705 as an outgroup, the proportion of fixed differences that is caused by either fixed
706 derived alleles in *P. tremula* or *P. tremuloides* among all segregating sites; the
707 proportion of inter-species shared polymorphisms among all segregating sites; and the
708 relative node depth (RND). RND was calculated by dividing the d_{xy} of the two aspen
709 species by d_{xy} between aspen (represented by 24 samples of *P. tremula* in this study)
710 and *P. trichocarpa* (24 samples; see (Wang, et al. unpublished data). Significance of
711 the differences between regions putatively under selection and the genome-wide
712 averages for all above mentioned population genetic statistics were examined using
713 one-sided Wilcoxon ranked-sum tests.
714

715 **Gene ontology (GO) enrichment**

716 To determine whether any functional classes of genes were overrepresented among
717 regions putatively under selection, we performed functional enrichment analysis of
718 gene ontology (GO) using Fisher's exact test by agriGO's Term Enrichment tool
719 (http://bioinfo.cau.edu.cn/agriGO/index.php; (Du, et al. 2010). GO groups with fewer
720 than two outlier genes were excluded from this analysis. *P*-values of Fisher's exact
721 test were further corrected for multiple testing with Benjamini-Hochberg false
722 discovery rate (Benjamini and Hochberg 1995). GO terms with a corrected *P*-value
723 <0.05 were considered to be significantly enriched.

724

725 ## Acknowledgements

726

727 We are grateful to Rick Lindroth for providing access to the samples of *P.*
728 *tremuloides* used in this study. We thank Carin Olofsson for extracting DNA for all
729 samples used in this study. The research has been funded through grants from
730 Vetenskapsrådet and a Young Researcher Award from Umeå University to PKI. JW
731 was supported by a scholarship from the Chinese Scholarship Council (No.
732 2011618053).

733

734 **References**

735

736 Avise JC. 2000. Phylogeography: the history and formation of species: Harvard
737 university press.

738 Barton N, Malik HS. 2010. Understanding Adaptation in Large Populations. PLoS
739 Genet 6:e1000987.

740 Begun DJ, Aquadro CF. 1992. Levels of naturally occurring DNA polymorphism
741 correlate with recombination rates in D. melanogaster. Nature 356:519-520.
742 Benjamini Y, Hochberg Y. 1995. Controlling the false discovery rate: a practical
743 and powerful approach to multiple testing. Journal of the Royal Statistical
744 Society. Series B (Methodological):289-300.
745 Burri R, Nater A, Kawakami T, Mugal CF, Olason PI, Smeds L, Suh A, Dutoit L,
746 Bureš S, Garamszegi LZ. 2015. Linked selection and recombination rate variation
747 drive the evolution of the genomic landscape of differentiation across the
748 speciation continuum of Ficedula flycatchers. Genome research:gr.
749 196485.196115.
750 Carneiro M, Albert F, Afonso S, Pereira R, Burbano H, Campos R, Melo-Ferreira J,
751 Blanco-Aguiar J, Villafuerte R, Nachman M. 2014. The Genomic Architecture of
752 Population Divergence between Subspecies of the European Rabbit. PLoS
753 genetics 10:e1003519.
754 Charlesworth B. 1998. Measures of divergence between populations and the
755 effect of forces that reduce variability. Molecular biology and evolution 15:538-
756 543.
757 Charlesworth D. 2006. Balancing selection and its effects on sequences in nearby
758 genome regions. PLoS Genet 2:e64.
759 Chikhi L, Sousa VC, Luisi P, Goossens B, Beaumont MA. 2010. The confounding
760 effects of population structure, genetic diversity and the sampling scheme on the
761 detection and quantification of population size changes. Genetics 186:983-995.
762 Comes HP, Kadereit JW. 1998. The effect of Quaternary climatic changes on plant
763 distribution and evolution. Trends in plant science 3:432-438.
764 Coyne JA, Orr HA. 2004. Speciation: Sinauer Associates Sunderland, MA.

765 Cruickshank TE, Hahn MW. 2014. Reanalysis suggests that genomic islands of
766 speciation are due to reduced diversity, not reduced gene flow. Molecular
767 ecology 23:3133-3157.
768 Danecek P, Auton A, Abecasis G, Albers CA, Banks E, DePristo MA, Handsaker RE,
769 Lunter G, Marth GT, Sherry ST. 2011. The variant call format and VCFtools.
770 Bioinformatics 27:2156-2158.
771 DePristo MA, Banks E, Poplin R, Garimella KV, Maguire JR, Hartl C, Philippakis
772 AA, Del Angel G, Rivas MA, Hanna M. 2011. A framework for variation discovery
773 and genotyping using next-generation DNA sequencing data. Nature genetics
774 43:491-498.
775 Du S, Wang Z, Ingvarsson PK, Wang D, Wang J, Wu Z, Tembrock LR, Zhang J.
776 2015. Multilocus Analysis of Nucleotide Variation and Speciation in Three
777 Closely Related Populus (Salicaceae) Species. Molecular ecology.
778 Du Z, Zhou X, Ling Y, Zhang Z, Su Z. 2010. agriGO: a GO analysis toolkit for the
779 agricultural community. Nucleic acids research 38:W64-W70.
780 Eckenwalder JE. 1996. Systematics and evolution of Populus. Biology of Populus
781 and its Implications for Management and Conservation:7-32.
782 Ellegren H, Smeds L, Burri R, Olason PI, Backström N, Kawakami T, Künstner A,
783 Mäkinen H, Nadachowska-Brzyska K, Qvarnström A. 2012. The genomic
784 landscape of species divergence in Ficedula flycatchers. Nature 491:756-760.
785 Excoffier L, Dupanloup I, Huerta-Sánchez E, Sousa V, Foll M. 2013. Robust
786 demographic inference from genomic and SNP data. PLoS genetics 9:e1003905.
787 Fay JC, Wu C-I. 2000. Hitchhiking under positive Darwinian selection. Genetics
788 155:1405-1413.

789 Feder JL, Xie X, Rull J, Velez S, Forbes A, Leung B, Dambroski H, Filchak KE, Aluja
790 M. 2005. Mayr, Dobzhansky, and Bush and the complexities of sympatric
791 speciation in Rhagoletis. Proceedings of the National Academy of Sciences
792 102:6573-6580.
793 Feulner P, Chain F, Panchal M, Huang Y, Eizaguirre C, Kalbe M, Lenz T, Samonte I,
794 Stoll M, Bornberg-Bauer E. 2015. Genomics of Divergence along a Continuum of
795 Parapatric Population Differentiation. PLoS genetics 11:e1004966.
796 Feulner PG, Chain FJ, Panchal M, Huang Y, Eizaguirre C, Kalbe M, Lenz TL,
797 Samonte IE, Stoll M, Bornberg-Bauer E. Genomics of divergence along a
798 continuum of parapatric population differentiation.
799 Fumagalli M, Vieira FG, Korneliussen TS, Linderoth T, Huerta-Sánchez E,
800 Albrechtsen A, Nielsen R. 2013. Quantifying population genetic differentiation
801 from next-generation sequencing data. Genetics 195:979-992.
802 Fumagalli M, Vieira FG, Linderoth T, Nielsen R. 2014. ngsTools: methods for
803 population genetics analyses from next-generation sequencing data.
804 Bioinformatics 30:1486-1487.
805 Gladenkov AY, Oleinik AE, Marincovich L, Barinov KB. 2002. A refined age for the
806 earliest opening of Bering Strait. Palaeogeography, Palaeoclimatology,
807 Palaeoecology 183:321-328.
808 Hamzeh M, Dayanandan S. 2004. Phylogeny of Populus (Salicaceae) based on
809 nucleotide sequences of chloroplast trnT-trnF region and nuclear rDNA.
810 American journal of botany 91:1398-1408.
811 Hermisson J, Pennings PS. 2005. Soft sweeps molecular population genetics of
812 adaptation from standing genetic variation. Genetics 169:2335-2352.

813 Hewitt G. 2004. Genetic consequences of climatic oscillations in the Quaternary.
814 Philosophical Transactions of the Royal Society of London B: Biological Sciences
815 359:183-195.
816 Hewitt G. 2000. The genetic legacy of the Quaternary ice ages. Nature 405:907-
817 913.
818 Hu A, Meehl GA, Otto-Bliesner BL, Waelbroeck C, Han W, Loutre M-F, Lambeck K,
819 Mitrovica JX, Rosenbloom N. 2010. Influence of Bering Strait flow and North
820 Atlantic circulation on glacial sea-level changes. Nature Geoscience 3:118-121.
821 Kamau E, Charlesworth D. 2005. Balancing selection and low recombination
822 affect diversity near the self-incompatibility loci of the plant Arabidopsis lyrata.
823 Current Biology 15:1773-1778.
824 Kaufman D, Manley W. 2004. Quaternary glaciations—Extent and chronology,
825 Part II: North America: Developments in Quaternary Science Volume 2.
826 Keinan A, Reich D, Begun DJ. 2010. Human population differentiation is strongly
827 correlated with local recombination rate. PLoS Genet 6:e1000886.
828 Kim SY, Lohmueller KE, Albrechtsen A, Li Y, Korneliussen T, Tian G, Grarup N,
829 Jiang T, Andersen G, Witte D. 2011. Estimation of allele frequency and
830 association mapping using next-generation sequencing data. BMC bioinformatics
831 12:231.
832 Koch MA, Haubold B, Mitchell-Olds T. 2000. Comparative evolutionary analysis of
833 chalcone synthase and alcohol dehydrogenase loci in Arabidopsis, Arabis, and
834 related genera (Brassicaceae). Molecular biology and evolution 17:1483-1498.
835 Korneliussen TS, Albrechtsen A, Nielsen R. 2014. ANGSD: analysis of next
836 generation sequencing data. BMC bioinformatics 15:356.

837 Leffler EM, Gao Z, Pfeifer S, Ségurel L, Auton A, Venn O, Bowden R, Bontrop R,
838 Wall JD, Sella G. 2013. Multiple instances of ancient balancing selection shared
839 between humans and chimpanzees. Science 339:1578-1582.
840 Li H. 2013. Aligning sequence reads, clone sequences and assembly contigs with
841 BWA-MEM. arXiv preprint arXiv:1303.3997.
842 Li H, Durbin R. 2011. Inference of human population history from individual
843 whole-genome sequences. Nature 475:493-496.
844 Li H, Handsaker B, Wysoker A, Fennell T, Ruan J, Homer N, Marth G, Abecasis G,
845 Durbin R. 2009. The sequence alignment/map format and SAMtools.
846 Bioinformatics 25:2078-2079.
847 Lohse M, Bolger A, Nagel A, Fernie AR, Lunn JE, Stitt M, Usadel B. 2012. RobiNA: a
848 user-friendly, integrated software solution for RNA-Seq-based transcriptomics.
849 Nucleic acids research:gks540.
850 Luikart G, England PR, Tallmon D, Jordan S, Taberlet P. 2003. The power and
851 promise of population genomics: from genotyping to genome typing. Nature
852 Reviews Genetics 4:981-994.
853 Marincovich L, Gladenkov AY. 1999. Evidence for an early opening of the Bering
854 Strait. Nature 397:149-151.
855 McVean GA, Myers SR, Hunt S, Deloukas P, Bentley DR, Donnelly P. 2004. The
856 fine-scale structure of recombination rate variation in the human genome.
857 Science 304:581-584.
858 Milne RI, Abbott RJ. 2002. The origin and evolution of Tertiary relict floras.
859 Advances in Botanical Research 38:281-314.

860 Morjan CL, Rieseberg LH. 2004. How species evolve collectively: implications of
861 gene flow and selection for the spread of advantageous alleles. Molecular ecology
862 13:1341-1356.
863 Müller A, Leuschner C, Horna V, Zhang C. 2012. Photosynthetic characteristics
864 and growth performance of closely related aspen taxa: on the systematic
865 relatedness of the Eurasian Populus tremula and the North American P.
866 tremuloides. Flora-Morphology, Distribution, Functional Ecology of Plants
867 207:87-95.
868 Nachman MW, Payseur BA. 2012. Recombination rate variation and speciation:
869 theoretical predictions and empirical results from rabbits and mice.
870 Philosophical Transactions of the Royal Society B: Biological Sciences 367:409-
871 421.
872 Neale DB, Kremer A. 2011. Forest tree genomics: growing resources and
873 applications. Nature Reviews Genetics 12:111-122.
874 Nei M. 1987. Molecular evolutionary genetics: Columbia university press.
875 Nielsen R, Korneliussen T, Albrechtsen A, Li Y, Wang J. 2011. SNP calling,
876 genotype calling, and sample allele frequency estimation from New-Generation
877 Sequencing data. PloS one 7:e37558.
878 Noor MA, Bennett SM. 2009. Islands of speciation or mirages in the
879 desert? Examining the role of restricted recombination in maintaining
880 species. Heredity 103:439-444.
881 Nosil P, Feder JL. 2012. Genomic divergence during speciation: causes and
882 consequences. Philosophical Transactions of the Royal Society B: Biological
883 Sciences 367:332-342.

884 Nosil P, Funk DJ, ORTIZ-BARRIENTOS D. 2009. Divergent selection and
885 heterogeneous genomic divergence. Molecular ecology 18:375-402.
886 Patterson N, Price A, Reich D. 2006. Population structure and eigenanalysis. PLoS
887 Genet 2:e190.
888 Pennings PS, Hermisson J. 2006. Soft sweeps III: the signature of positive
889 selection from recurrent mutation. PLoS Genet 2:e186.
890 Pregitzer KS, Barnes BV. 1980. Flowering phenology of Populus tremuloides and
891 P. grandidentata and the potential for hybridization. Canadian Journal of Forest
892 Research 10:218-223.
893 Pritchard JK, Di Rienzo A. 2010. Adaptation–not by sweeps alone. Nature
894 Reviews Genetics 11:665-667.
895 Pritchard JK, Pickrell JK, Coop G. 2010. The genetics of human adaptation: hard
896 sweeps, soft sweeps, and polygenic adaptation. Current Biology 20:R208-R215.
897 Renaut S, Grassa C, Yeaman S, Moyers B, Lai Z, Kane N, Bowers J, Burke J,
898 Rieseberg L. 2013. Genomic islands of divergence are not affected by geography
899 of speciation in sunflowers. Nature Communications 4:1827.
900 Salvaudon L, Giraud T, Shykoff JA. 2008. Genetic diversity in natural populations:
901 a fundamental component of plant–microbe interactions. Current opinion in
902 plant biology 11:135-143.
903 Scheet P, Stephens M. 2006. A fast and flexible statistical model for large-scale
904 population genotype data: applications to inferring missing genotypes and
905 haplotypic phase. The American Journal of Human Genetics 78:629-644.
906 Schiffels S, Durbin R. 2014. Inferring human population size and separation
907 history from multiple genome sequences. Nature genetics 46:919-925.

908 Schrider DR, Mendes FK, Hahn MW, Kern AD. 2015. Soft shoulders ahead:
909 spurious signatures of soft and partial selective sweeps result from linked hard
910 sweeps. Genetics 200:267-284.
911 Seehausen O, Butlin RK, Keller I, Wagner CE, Boughman JW, Hohenlohe PA,
912 Peichel CL, Saetre G-P, Bank C, Brännström Å. 2014. Genomics and the origin of
913 species. Nature Reviews Genetics 15:176-192.
914 Skotte L, Korneliussen TS, Albrechtsen A. 2013. Estimating individual admixture
915 proportions from next generation sequencing data. Genetics 195:693-702.
916 Slatkin M. 1985. Gene flow in natural populations. Annual review of ecology and
917 systematics:393-430.
918 Smith JM, Haigh J. 1974. The hitch-hiking effect of a favourable gene. Genetical
919 research 23:23-35.
920 Sousa V, Hey J. 2013. Understanding the origin of species with genome-scale
921 data: modelling gene flow. Nature Reviews Genetics 14:404-414.
922 Strasburg JL, Sherman NA, Wright KM, Moyle LC, Willis JH, Rieseberg LH. 2012.
923 What can patterns of differentiation across plant genomes tell us about
924 adaptation and speciation? Philosophical Transactions of the Royal Society B:
925 Biological Sciences 367:364-373.
926 Tajima F. 1989. Statistical method for testing the neutral mutation hypothesis by
927 DNA polymorphism. Genetics 123:585-595.
928 Tarailo-Graovac M, Chen N. 2009. Using RepeatMasker to Identify Repetitive
929 Elements in Genomic Sequences. Current Protocols in Bioinformatics 4:1-4.10.
930 Tiffin P, Moeller DA. 2006. Molecular evolution of plant immune system genes.
931 Trends in genetics 22:662-670.

932 Tullus A, Rytter L, Tullus T, Weih M, Tullus H. 2012. Short-rotation forestry with
933 hybrid aspen (Populus tremula L.× P. tremuloides Michx.) in Northern Europe.
934 Scandinavian Journal of Forest Research 27:10-29.
935 Turner T, Hahn M, Nuzhdin S. 2005. Genomic islands of speciation in Anopheles
936 gambiae. PLoS Biol 3:e285.
937 Turner TL, Hahn MW. 2010. Genomic islands of speciation or genomic islands
938 and speciation? Molecular ecology 19:848-850.
939 Tuskan G, Difazio S, Jansson S, Bohlmann J, Grigoriev I, Hellsten U, Putnam N,
940 Ralph S, Rombauts S, Salamov A. 2006. The genome of black cottonwood,
941 Populus trichocarpa (Torr. & Gray). Science 313:1596-1604.
942 Via S. 2009. Natural selection in action during speciation. Proceedings of the
943 National Academy of Sciences 106:9939-9946.
944 Wang J, Scofield D, Street N, Ingvarsson P. 2015. Variant calling using NGS data in
945 European aspen (Populus tremula).
946 Wang J, Street NR, Scofield DG, Ingvarsson PK. unpublished data. Comparative
947 population genomics of three related Populus species. bioRxiv:026344.
948 Wang Z, Du S, Dayanandan S, Wang D, Zeng Y, Zhang J. 2013. Phylogeny
949 reconstruction and hybrid analysis of populus (salicaceae) based on nucleotide
950 sequences of multiple single-copy nuclear genes and plastid fragments. PloS one
951 9:e103645.
952 White BJ, Cheng C, Simard F, Costantini C, Besansky NJ. 2010. Genetic association
953 of physically unlinked islands of genomic divergence in incipient species of
954 Anopheles gambiae. Molecular ecology 19:925-939.

955 Wittkopp PJ, Kalay G. 2012. Cis-regulatory elements: molecular mechanisms and
956 evolutionary processes underlying divergence. Nature Reviews Genetics 13:59-
957 69.
958 Wolf JB, Lindell J, Backström N. 2010. Speciation genetics: current status and
959 evolving approaches. Philosophical Transactions of the Royal Society of London
960 B: Biological Sciences 365:1717-1733.
961
962
963
964
965
966
967
968
969
970
971
972
973
974
975
976
977
978

979 **Figures and Tables**

980

981 **Figure 1**. **Geographic distribution and genetic structure of 24 *Populus tremula***
982 **and 22 *P. tremuloides*.** (a) Map showing the current geographic distribution of *P.*
983 *tremula* (red) and *P. tremuloides* (blue). Yellow circles and triangles indicate the
984 locations where the 24 individuals of *P. tremula* and 22 individuals of *P. tremuloides*
985 were sampled. (b) Genetic structure of the two aspen species inferred using
986 NGSadmix. The y-axis quantifies subgroup membership, and the x-axis shows the
987 sample ID for each individual. (c) Principal component analysis (PCA) plot based on
988 genetic covariance among all individuals of *P. tremula* (red circle) and *P. tremuloides*
989 (green square and blue triangle). The first two principle components (PCs) are shown,
990 with PC1 explaining 21.04% (P=2.51×10^{-19}, Tacey-Widom test) of the overall genetic
991 variation and separating the two species and PC2 explaining 2.09% (P=9.65×10^{-4},
992 Tracy-Widom test) of the overall variation and separating the Wisconsin samples
993 (blue triangle) of *P. tremloides* from Alberta (green square). (d) Pie chart
994 summarizing the proportion of fixed, shared and exclusive polymorphisms of the two
995 aspen species.

996

997 **Figure 2**. **Demographic history of *Populus tremula* and *P. tremuloides*.** (a)
998 Graphical summary of the most likely inferred demographic scenario of speciation
999 implemented in *fastsimcoal2*. (b) Multiple sequential Markovian coalescent (MSMC)
1000 estimates of the effective population size (N_e) changes for *P. tremula* (red line) and *P.*
1001 *tremuloides* (blue line) based on the inference from two (dashed), four (dotted) and
1002 eight (solid) phased haplotypes. Time scale on the x-axis is calculated assuming a

1003 neutral mutation rate per generation (μ) = 3.75×10^{-8} and generation time (g) = 15
1004 years. The grey bar indicates the speciation time inferred by *fastsimcoal2*.
1005
1006 **Figure 3. Illustration of the strategy for detecting candidate regions under**
1007 **selection.** (a) Frequency histogram of the distribution of F_{ST} values over 10 Kbp non-
1008 overlapping windows across the genome. Data points located to the left (F_{ST}=0.169)
1009 and right (F_{ST}=0.681) vertical dashed lines (corresponding to the bottom and top 2.5%
1010 of the empirical F_{ST} distribution) were identified as regions with exceptional low and
1011 high differentiation between *P. tremula* and *P. tremuloides*. (b) For windows with
1012 exceptional high differentiation between species, two steps of filtering were
1013 performed. In step1, we filtered windows where d_{xy} was smaller than the genome-
1014 wide median value. In step 2, the bottom 5% thresholds (short dashed lines) of
1015 nucleotide diversity (θ_π) was applied to classify divergent windows into four mutually
1016 exclusive categories: hard selective sweeps occurred in both species (black dots) if θ_π
1017 dropped below the bottom 5% of empirical distribution in both species; hard sweeps
1018 occurred in only one of *P. tremula* (red dots) and *P. tremuloides* (blue dots) if θ_π
1019 dropped below the bottom 5% of empirical distribution only in the respective species;
1020 adaptation occurred from standing genetic variation (soft selective sweeps, grey dots)
1021 if θ_π appeared similar as background (not below the threshold). In both (b) and (c) the
1022 long dashed lines indicate the genome-wide median values of θ_π in *P. tremula* and *P.*
1023 *tremuloides*, respectively. (c) For windows with exceptional low differentiation
1024 between species, we performed two filtering steps to identify regions potentially
1025 under long-term balancing selection. In step1, we filtered windows where the
1026 coverage breadth was lower than 3 Kbp. In step2, only windows where θ_π was above
1027 the top 5% of empirical distributions (short dashed lines) in both species were

1028 considered as being under long-term balancing selection (green dots). Please refer to
1029 Table 2 for the proportion and other genomic features for each category.
1030
1031 **Figure 4. Genome-wide divergence.** Chromosomal distribution of genetic
1032 differentiation (F_{ST}) between *Populus tremula* and *P. tremuloides*. The small, light
1033 blue dots indicate F_{ST} values estimated over 10 Kbp non-overlapping windows. Grey
1034 lines indicate F_{ST} values estimated over 100 Kbp non-overlapping windows.
1035 Locations for windows showing specific signatures of selection are highlighted with
1036 colored bars above the plot. Among them, candidate windows under hard selective
1037 sweeps in either one or both species (red, blue and black bars) are located on the
1038 topside; candidate windows with signatures of soft sweeps in either one or both
1039 species (grey bars) are located in the middle; and candidate windows under long-term
1040 balancing selection (green bars) in both species are located at the bottom of all bars.
1041
1042 **Figure 5. Comparisons of recombination rates (ρ/θ_π) between selected regions**
1043 **and genomic background in *P. tremula* (a) and *P. tremuloides* (b).** Black, red, blue,
1044 grey, green and light blue boxplots represent ρ/θ_π within regions with signatures of
1045 hard sweeps in both species, only in *P. tremula*, only in *P. tremuloides*, soft sweeps in
1046 either one or both species, long-term balancing selection and the rest of the genome,
1047 respectively. Asterisks designate significant differences between candidate regions
1048 with signatures of selection and the rest of genomic regions by Mann-Whitney U test
1049 (* *P*-value < 0.05; ** *P*-value < 1e-4; ***P-value <2.2e-16).
1050
1051 **Table 1**. Inferred demographic parameters of the divergence history between *P.*
1052 *tremula* and *P. tremuloides* for the best model shown in Figure 2a.

1053

Parameters	Point estimation	95% CI[a] Lower bound	Upper bound
N_{ANC}	56235	48012	69492
$N_{P.tremula}$	102814	93688	105671
$N_{P.tremuloides}$	309500	247321	310105
$2Nm_{P.tremuloides->P.tremula}$	0.202	0.156	0.375
$2Nm_{P.tremula->P.tremuloides}$	0.053	0.052	0.117
T_{DIV}	2332410	2186760	3113520

1054

1055 Parameters are defined in Figure 2a. N indicates the effective population size of *P. tremula*, *P.*
1056 *tremuloides* or their ancestral population, m indicates the migration rates between species on either
1057 direction, T_{DIV} indicates the estimated divergence time between the two species from *fastsimcoal* 2.
1058 [a]Parametric bootstrap estimates obtained by parameter estimation from 100 data sets simulated
1059 according to the overall maximum composite likelihood estimates shown in point estimation columns.
1060 Estimation were obtained from 100,000 simulations per likelihood.

1061

1062

1063

1064

1065

1066

1067

1068 **Table 2. Summary statistics charactering selected regions in both *P. tremula* and**
1069 ***P. tremuloides*.**

1070

Parameters	Species	Both[a] (5.87%)	*P. tremula*[a] (12.61%)	*P. tremuloides*[a] (8.26%)	Soft[a] (73.26%)	Balancing[a]	Background[a]
θπ	*P. tremula*	0.0039***	0.0046***	0.0092**	0.0112***	0.0404***	0.0147
	P. tremuloides	0.0054***	0.0103**	0.0059***	0.0133**	0.0422***	0.0159
Tajima's D	*P. tremula*	-1.2763***	-1.2731***	-0.6377**	-0.7137***	0.2433**	-0.3016
	P. tremuloides	-1.9246***	-1.4904**	-1.8498***	-1.4244***	-0.2711***	-1.1606
Fay&Wu'sH	*P. tremula*	-0.6659**	-0.8390***	-0.6167**	-0.7786***	-0.0986**	-0.4008
	P. tremuloides	-0.3908*	-0.4265**	-0.5809**	-0.6168***	-0.0954**	-0.3236
r^2	*P. tremula*	0.2796*	0.2700**	0.2786**	0.2571**	0.1718*	0.2115
	P. tremuloides	0.2894**	0.2336**	0.2250**	0.2202**	0.1393	0.1575
Fixed (%)	*P. tremula*	0.0997***	0.0609***	0.0625***	0.0470***	~0**	0.0055
	P. tremuloides	0.0767***	0.0349***	0.0644***	0.0372***	~0**	0.0035
Shared (%)		0.0487***	0.0688***	0.0727***	0.1001***	0.3718***	0.1662
F_{ST}		0.8280***	0.7447***	0.7544***	0.7258***	0.1330***	0.3836
d_{xy}		0.0270*	0.0297**	0.0309**	0.0448***	0.0468***	0.0248
RND		0.8404**	0.7527***	0.7789**	0.8105***	0.7614***	0.5509

1071 [a]Both indicates candidate regions with signatures of hard selective sweeps in both species; *P. tremula*
1072 and *P. tremuloides* indicate candidate regions with signatures of hard sweeps only in the respective
1073 species; Soft indicates candidate regions with signatures of soft sweeps in either one or both species;
1074 Balancing indicates candidate regions with signatures of long-standing balancing selection in both
1075 species. Background indicates the rest of the genome not showing exceptional differentiation. Asterisks
1076 designate significant differences between the regions under selection and the rest of genomic regions
1077 by Mann-Whitney U test (* *P*-value < 0.05; ** *P*-value < 1e-4; ***P-value <2.2e-16).

1078

1079

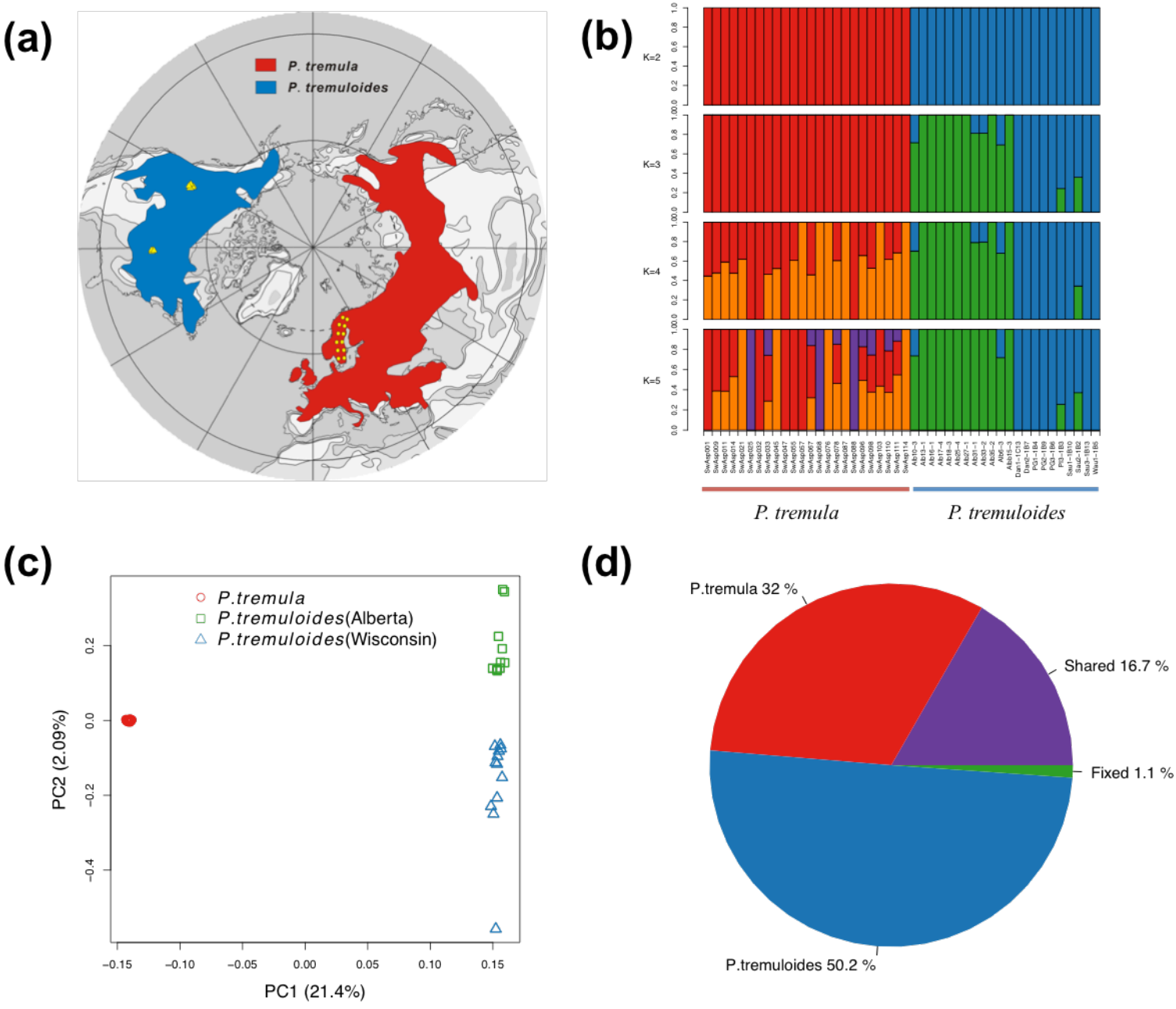
(a)
P. tremula
P. tremuloides
(b)
K=2
K=3
K=4
K=5
P. tremula
P. tremuloides
(c)
P.tremula
P.tremuloides(Alberta)
P.tremuloides(Wisconsin)
PC2 (2.09%)
PC1 (21.4%)
(d)
P.tremula 32 %
Shared 16.7 %
Fixed 1.1 %
P.tremuloides 50.2 %

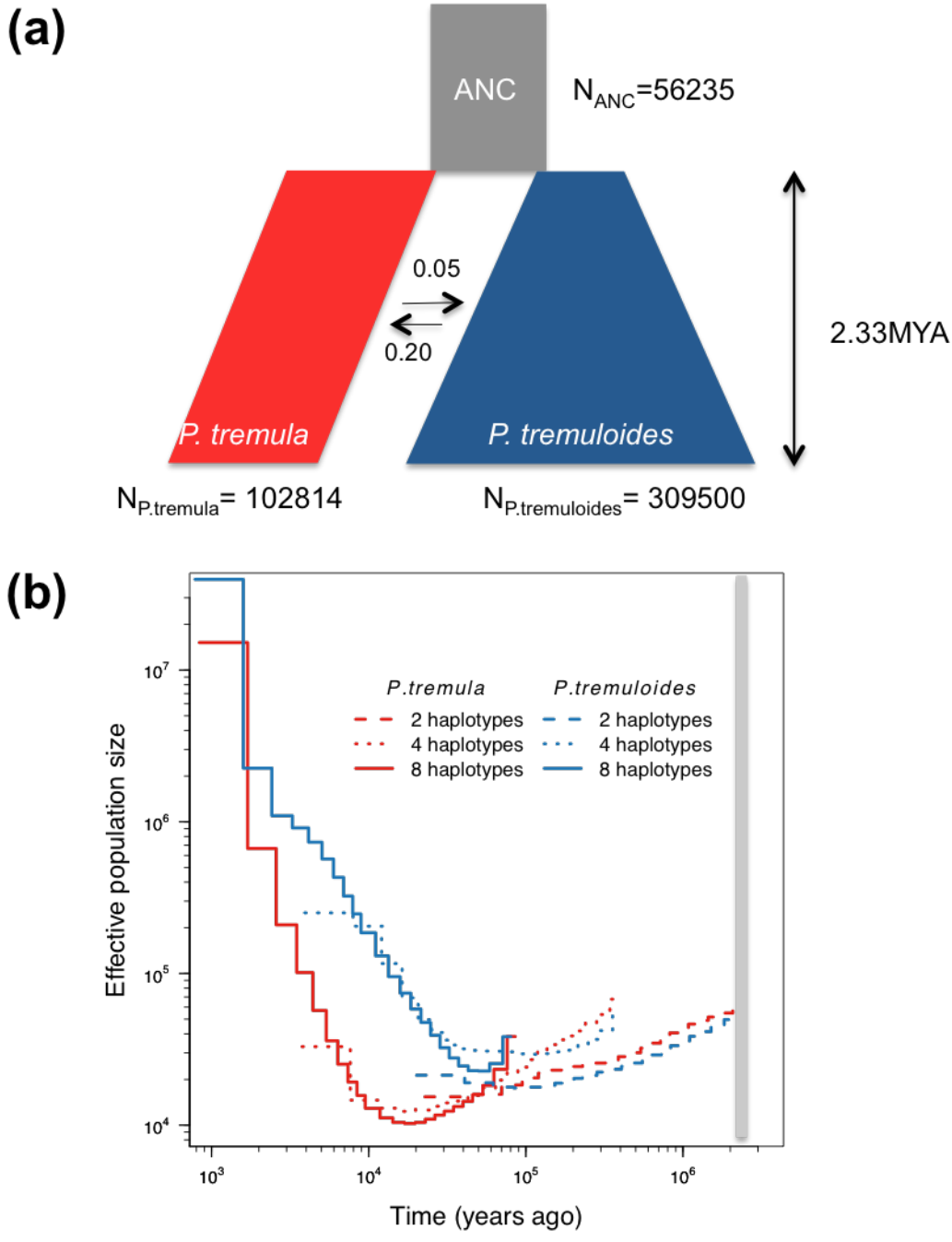
(a)
ANC
N_ANC=56235
0.05
0.20
2.33MYA
P. tremula
P. tremuloides
N_P.tremula= 102814
N_P.tremuloides= 309500
(b)
P.tremula
2 haplotypes
4 haplotypes
8 haplotypes
P.tremuloides
2 haplotypes
4 haplotypes
8 haplotypes
Effective population size
Time (years ago)

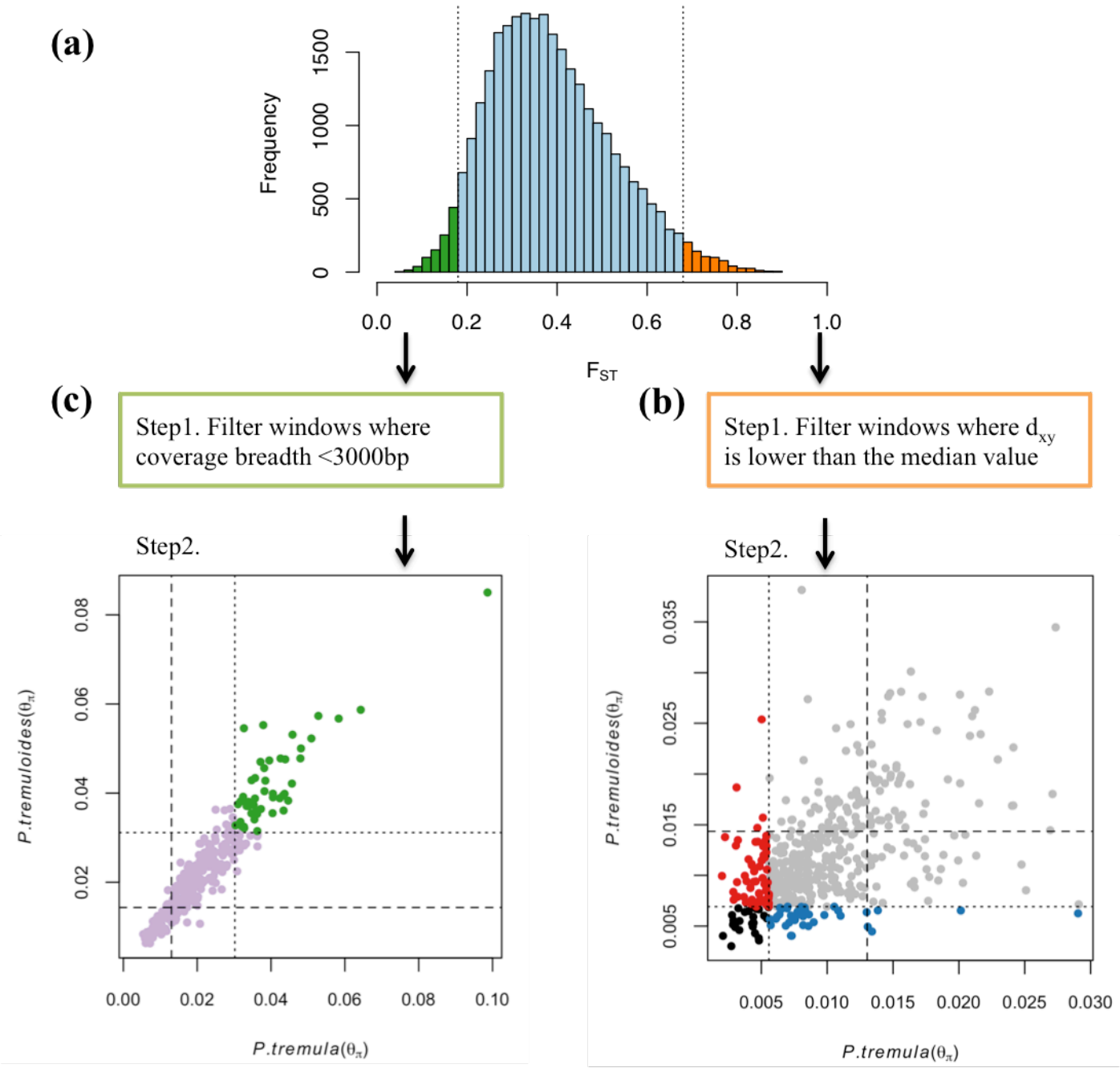
(a)
Frequency
0
500
1000
1500
0.0
0.2
0.4
0.6
0.8
1.0
F_{ST}
(c)
Step1. Filter windows where coverage breadth <3000bp
Step2.
P.tremuloides(θ_π)
0.02
0.04
0.06
0.08
0.00
0.02
0.04
0.06
0.08
0.10
P.tremula(θ_π)
(b)
Step1. Filter windows where d_{xy} is lower than the median value
Step2.
P.tremuloides(θ_π)
0.005
0.015
0.025
0.035
0.005
0.010
0.015
0.020
0.025
0.030
P.tremula(θ_π)

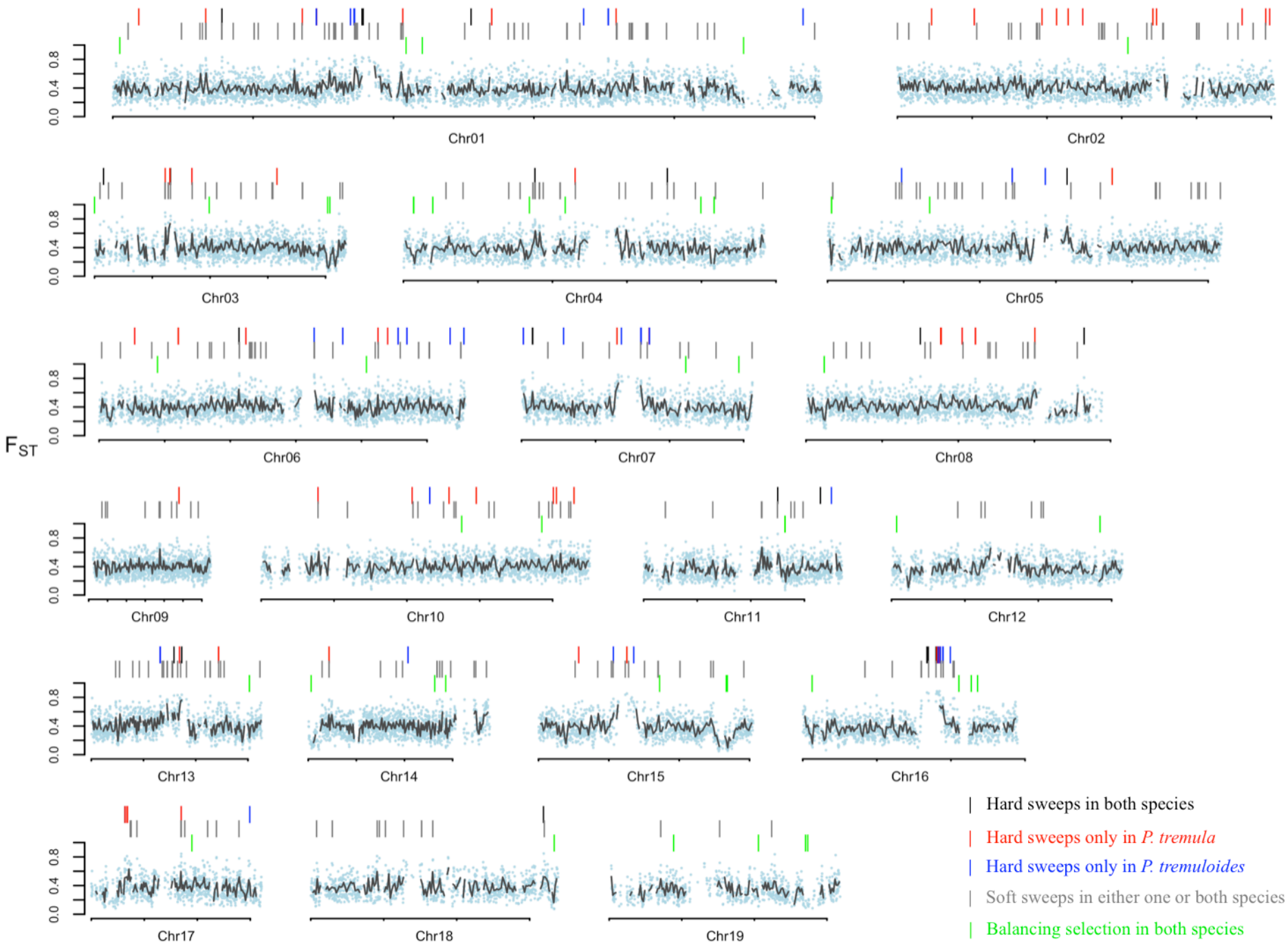
F_{ST}
0.0
0.4
0.8
Chr01
Chr02
Chr03
Chr04
Chr05
Chr06
Chr07
Chr08
Chr09
Chr10
Chr11
Chr12
Chr13
Chr14
Chr15
Chr16
Chr17
Chr18
Chr19
Hard sweeps in both species
Hard sweeps only in *P. tremula*
Hard sweeps only in *P. tremuloides*
Soft sweeps in either one or both species
Balancing selection in both species

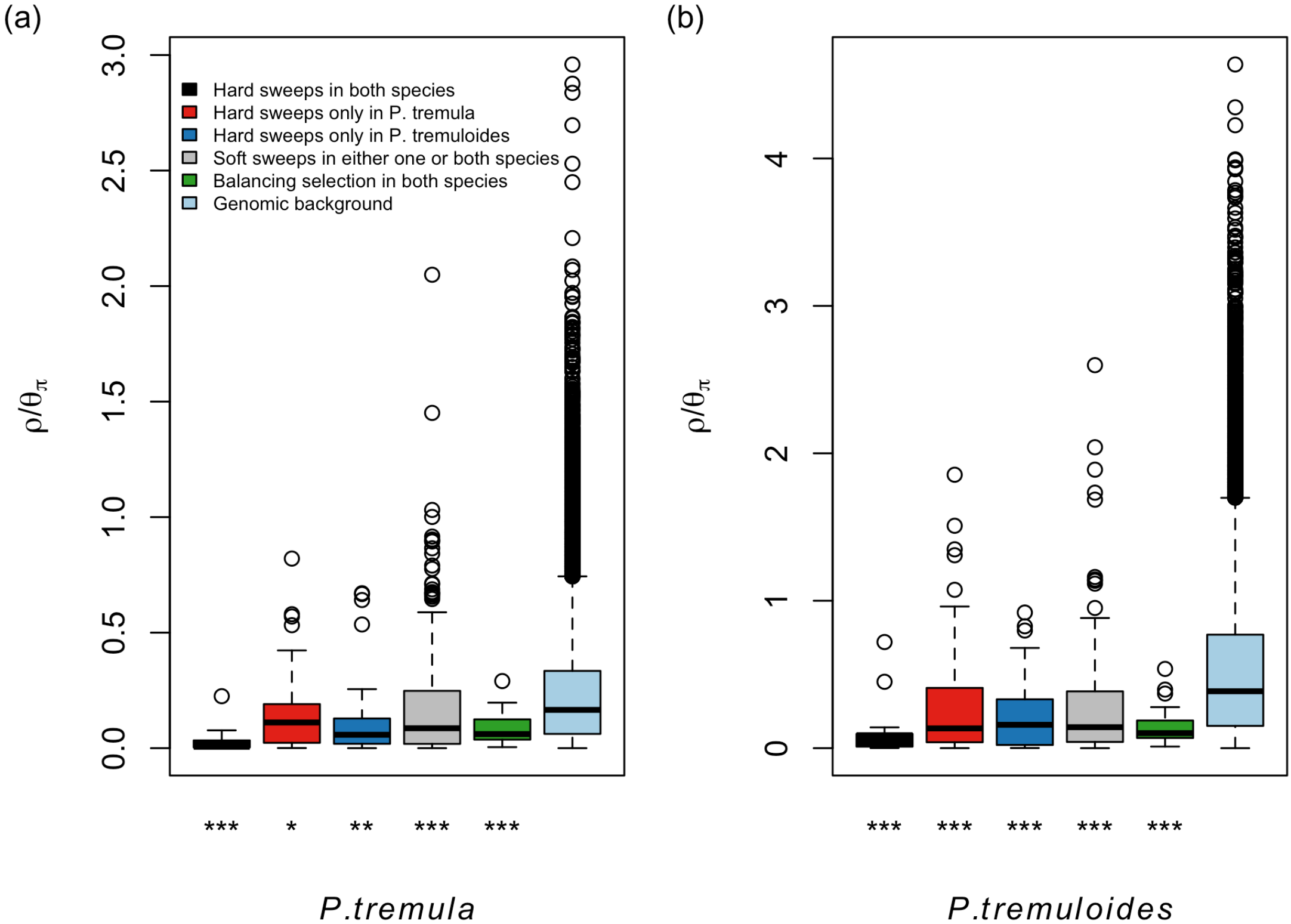
(a)
(b)
Hard sweeps in both species
Hard sweeps only in P. tremula
Hard sweeps only in P. tremuloides
Soft sweeps in either one or both species
Balancing selection in both species
Genomic background
ρ/θπ
0.0
0.5
1.0
1.5
2.0
2.5
3.0
0
1
2
3
4
***
*
**
***
***
***
***
***
***
***
P.tremula
P.tremuloides